2012 12th IEEE-RAS International Conference on Humanoid Robots
Nov.29-Dec.1, 2012. Business Innovation Center Osaka, Japan

Balance Control based on Capture Point Error Compensation for Biped Walking on Uneven Terrain

Mitsuharu Morisawa, Shuuji Kajita, Fumio Kanehiro, Kenji Kaneko, Kanako Miura and Kazuhiro Yokoi

***Abstract*—This paper tries to improve a balance control based on the Capture Point (CP) control. First the characteristics of the conventional balance controller are shown to be essentially the same as the CP controller. Then we analyze the transfer function of the balance controller. We introduce a new state variable with the CP integration to the CP and the ZMP (Zero-Moment Point) in order to trim a long term offset of the CP and the ZMP. Verification of the proposed balance controller is conducted through both simulation and experiments with a humanoid robot HRP-2[11].**

I. Introduction

Humanoid robots are expected to take over human's work in hazardous situations. The greatest hurdle is their mobile ability, which is still poorer than humans. Considering the above, the key technologies of biped locomotion are as follows: how to walk faster, how to save walking energy, and how to prevent a falling down. We give high priority to the last one because falling may cause a fatal damage on a robot.

There are various studies that have addressed this issue. Nishiwaki et al. [1] applied a preview control for online walking pattern generator to play the role of a long term stabilizer. Choi et al. [2] presented a stability proof by using the Lyapunov method for a balance control. Wieber [3] proposed the integration scheme of the COG motion with an adaptive footstep using Model Predictive Control under the linear inequality constraints. Sugihara [4] evaluated the stable pole of an inverted pendulum which maximizes the stable standing region using a method similar to the CP. Kajita et al. [5] proposed tracking control of a linear inverted pendulum for stabilization of a biped walking which balance controller is based on a state feedback of the COG and the ZMP considering a ZMP lag. Its ZMP lag was compensated in [6].

Pratt et al. [7] presented the *Capture Point* (CP) which leads a motion of the COG (Center of Gravity) to a complete stop. Takenaka et al. [8] had also focused on a divergent component which is equivalent to the CP of an inverted pendulum dynamics. A landing position is modified to prevent losing a balance according to a divergent component as a result of the *model ZMP control* which accelerates the upper body.

Mitsuharu Morisawa, Shuuji Kajita, Fumio Kanehiro, Kenji Kaneko, Kanako Miura and Kazuhito Yokoi are with Research Institute of Intelligent Systems, National Institute of Advanced Industrial Science and Technology (AIST), 1-1-1, Umezono, Tsukuba, Ibaraki, 305-8568, Japan. m.morisawa@aist.go.jp

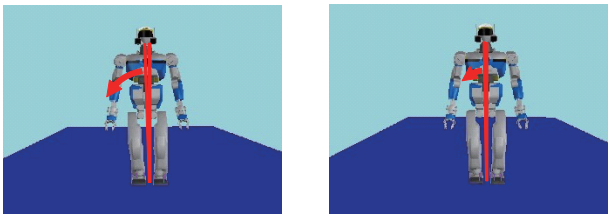

(a) without CP integration (conventional) (b) with CP integration (proposed)

Fig. 1. Posture error under presence of COG measurement error

Englsberger et al. [9] introduced two approaches for Capture Point control as balance control.

This paper focuses on a balance control of biped walking on uneven terrain. Under presence of the COG measurement error, the large offset of the COG position remains as can be seen in Fig.1. From a long-term point of view for a stable walking, a biped locomotion with a larger offset is easier to fall down. Thus, the CP integration is introduced to solve this problem. We try to improve a balance controller based on the similar type of the Capture Point control [9]. First the characteristics of the conventional balance controller is shown to be essentially the same as the CP controller. Then we analyze the transfer function of the balance controller in Sec.II. We introduce a new state variable that includes CP integration into the CP and the ZMP for an elimination of a long term offset of the CP and the ZMP in Sec.III. The validity of the proposed balance controller is evaluated through the simulations and the experiments in Sec.IV.

II. Balance Control using an Inverted Pendulum Model

A. Inverted Pendulum Model

With increasing walking speed, it is likely that the projected point of the center of gravity (COG) to the floor passes through the outside of the support polygon. An inverted pendulum model has been widely used for both the COG walking motion and a balance control[1]-[12] in order to reduce calculation costs. This paper also designs a balance controller using an inverted pendulum as shown in Fig.2. To control both the COG and the ZMP, differentiation of the ZMP $\dot{p}_x$ is set as input so that the state vector consists of

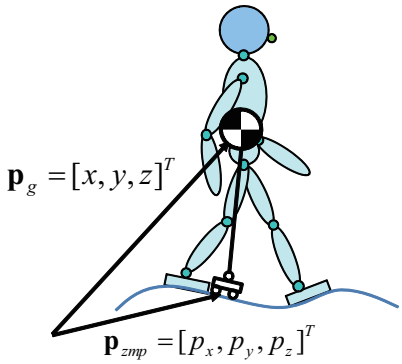

Fig. 2. Inverted Pendulum Model

the COG and the ZMP.

$$\frac{\mathrm{d}}{\mathrm{d}t}\begin{bmatrix} x \\ \dot{x} \\ p_x \end{bmatrix} = \begin{bmatrix} 0 & 1 & 0 \\ \omega^2 & 0 & -\omega^2 \\ 0 & 0 & 0 \end{bmatrix}\begin{bmatrix} x \\ \dot{x} \\ p_x \end{bmatrix} + \begin{bmatrix} 0 \\ 0 \\ 1 \end{bmatrix}\dot{p}_x, \quad (1)$$

where ω is the natural frequency of the inverted pendulum defined as

$$\omega \equiv \sqrt{\frac{g+\ddot{z}}{z-p_z}}.$$

The natural frequency ω is composed of the COG height z and gravity constant g. The height of the ZMP position p_z is traversed between the supported soles as well as the horizontal ZMP position. In this paper, the constant height of the COG is used in order to catch the control characteritics easily.

In our target humanoid robot HRP-2[11], elastic materials are attatched below the force sensor on the ankle in order to protect against a large impact force. We assume that the ZMP dynamics can be represented as a first order lag with new ZMP input p_x^d [5] which is approximated model as a force control characteristics of sole in more inner control loop and joint servo delay, and etc.

$$\dot{p}_x = -g_p p_x + g_p p_x^d \quad (2)$$

From (1) and (2), the system with the ZMP lag can be expressed as follows

$$\frac{\mathrm{d}}{\mathrm{d}t}\begin{bmatrix} x \\ \dot{x} \\ p_x \end{bmatrix} = \begin{bmatrix} 0 & 1 & 0 \\ \omega^2 & 0 & -\omega^2 \\ 0 & 0 & -g_p \end{bmatrix}\begin{bmatrix} x \\ \dot{x} \\ p_x \end{bmatrix} + \begin{bmatrix} 0 \\ 0 \\ g_p \end{bmatrix} p_x^d \quad (3)$$

B. COG and ZMP control

Let us consider to control both the COG and the ZMP. The feedback controller for the target system with the ZMP lag in (3) can be given as follows.

$$p_x^d = -k_1^{cz} x - k_2^{cz}\dot{x} - k_3^{cz} p_x, \quad (4)$$

where k_1^{cz},k_2^{cz},k_3^{cz} are the feedback gains. The feedback gains can be designed by the poles $(\alpha, \beta, \gamma < 0)$.

$$\begin{bmatrix} k_1^{cz} \\ k_2^{cz} \\ k_3^{cz} \end{bmatrix} = \begin{bmatrix} \frac{\alpha\beta\gamma+\omega^2(\alpha+\beta+\gamma)}{\omega^2 g_p} \\ -\frac{\alpha\beta+\beta\gamma+\gamma\alpha+\omega^2}{\omega^2 g_p} \\ -\frac{\alpha+\beta+\gamma+g_p}{g_p} \end{bmatrix} \quad (5)$$

Based on the best COG-ZMP regulator presented by Sugihara[4], the stable pole of the inverted pendulum provides the maximum stable standing region. Therefore, one of the poles γ is assigned to $-\omega$:

$$\begin{bmatrix} k_1^{cz} \\ k_2^{cz} \\ k_3^{cz} \end{bmatrix} = \begin{bmatrix} -\frac{(\alpha-\omega)(\beta-\omega)}{\omega g_p} \\ -\frac{(\alpha-\omega)(\beta-\omega)}{\omega^2 g_p} \\ -\frac{\alpha+\beta+g_p-\omega}{g_p} \end{bmatrix}. \quad (6)$$

C. Capture Point and ZMP control

The Capture Point(CP) ξ_x is defined as a convergence position of the COG at infinite time.

$$\xi_x = x + \frac{\dot{x}}{\omega} \quad (7)$$

The dynamics of the inverted pendulum can be represented by both the CP ξ_x and the ZMP p_x.

$$\dot{\xi}_x = \dot{x} + \frac{\ddot{x}}{\omega} = \omega(\xi_x - p_x) \quad (8)$$

From (2) and (8), the system equation can be expressed as:

$$\frac{\mathrm{d}}{\mathrm{d}t}\begin{bmatrix} \xi_x \\ p_x \end{bmatrix} = \begin{bmatrix} \omega & -\omega \\ 0 & -g_p \end{bmatrix}\begin{bmatrix} \xi_x \\ p_x \end{bmatrix} + \begin{bmatrix} 0 \\ g_p \end{bmatrix} p_x^d \quad (9)$$

The system in (9) also becomes controllable. The CP controller is proposed by Englsberger[9] and, the CP controller without the COG controller also could stabilize a biped robot. In this method, the CP controller and the ZMP controller were designed independently. We will design a balance controller for the both of the CP and the ZMP to clearly define the control performance. Here, let us consider the following feedback controller:

$$p_x^d = -k_1^{cp}\xi_x - k_2^{cp} p_x, \quad (10)$$

where k_1^{cp} and k_2^{cp} are the feedback gains. The relation between these feedback gains and the pole becomes

$$\begin{bmatrix} k_1^{cp} \\ k_2^{cp} \end{bmatrix} = \begin{bmatrix} -\frac{(\alpha-\omega)(\beta-\omega)}{\omega g_p} \\ -\frac{\alpha+\beta+g_p-\omega}{g_p} \end{bmatrix}. \quad (11)$$

By comparison of the COG-ZMP feedback gain in (6) with the CP feedback gain in (11),

$$\begin{aligned} k_1^{cp} &= k_1^{cz} = \omega k_2^{cz}, \\ k_2^{cp} &= k_3^{cz}, \end{aligned}$$

can be obviously found. Thus, the COG-ZMP controller in (4) which one of the poles is assigned to a natural frequency

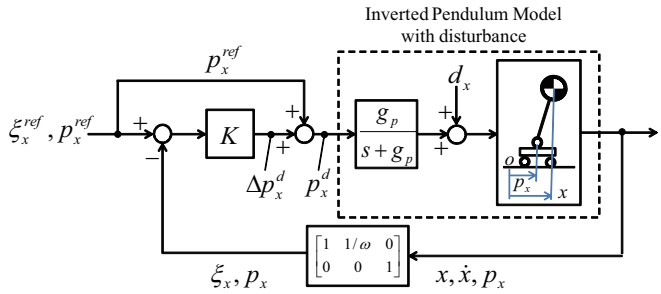

Fig. 3. Tracking controller of linear inverted pendulum[5]

of the inverted pendulum, provides completely the same output as the CP-ZMP controller.

$$\begin{aligned} p_x^d &= -k_1^{cz}x - k_2^{cz}\dot{x} - k_3^{cz}p_x, \\ &= -k_1^{cp}\left(x + \frac{\dot{x}}{\omega}\right) - k_2^{cp}p_x \end{aligned} \tag{12}$$

D. Characteritics of CP-ZMP controller

We suppose that a disturbance d_x affects the ZMP input of the system. The Capture Point (CP) dynamics under the presence of a disturbance is represented as

$$\dot{\xi}_x = \dot{x} + \frac{\ddot{x}}{\omega} = \omega(\xi_x - p_x + d_x). \tag{13}$$

In order to improve a tracking performance against the desired trajectory, the tracking controller of a linear inverted pendulum proposed by Kajita[5] is applied. In this method, the controller compensates the state error and the feedforward term of the ZMP is inserted to the output of the controller. This block diagram of the tracking control system is shown in Fig.3. We consider the state variables of the system in (10) to determine the state errors of the CP and the ZMP.

$$\Delta p_x^d = -k_1^{cp}(\xi_x - \xi_x^{ref}) - k_2^{cp}(p_x - p_x^{ref}) \tag{14}$$

ξ_x^{ref} and p_x^{ref} are the desired CP and ZMP trajectories respectively. The input to the system is generated from the sum of the controller output Δp_x^d and the desired ZMP reference p_x^{ref}.

$$p_x^d = p_x^{ref} + \Delta p_x^d \tag{15}$$

Then, control performance is analyzed in a frequency domain. Applying the CP-ZMP controller in (14) into the target system with the ZMP lag in (13), the transfer function of the CP and the ZMP from the input to the output can be derived by Laplace transformation.

$$\begin{aligned} \Xi_x(s) &= \frac{(\alpha-\omega)(\beta-\omega)}{(s-\alpha)(s-\beta)}\Xi_x^{ref}(s) \\ &+ \frac{\omega(\alpha+\beta-\omega)}{(s-\alpha)(s-\beta)}P_x^{ref}(s) \\ &+ \frac{\omega(s+g_p)}{(s-\alpha)(s-\beta)}D_x(s) \end{aligned} \tag{16}$$

$$P_x(s) = -\left(\frac{s-\omega}{\omega}\right)\Xi_x(s) \tag{17}$$

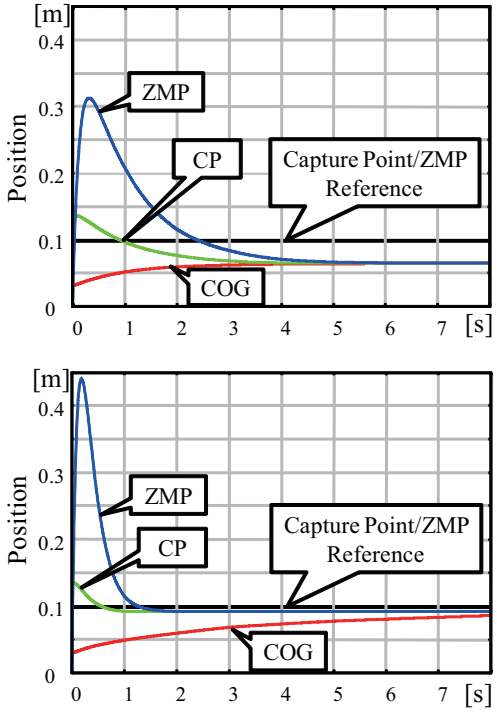

Fig. 4. Step response by CP controller under presence of disturbance for Pole assignment $\{\alpha, \beta\} = (\text{top} : \{-1, -8\}/\text{bottom} : \{-4, -8\})$, $\omega = \sqrt{g/0.8}$, $g_p = 20$ $[x(0), \dot{x}(0), p_x(0)]^T = [0.03, 0.03, 0]^T$ as initial value, $\xi_x^{ref} = p_x^{ref} = 0.1$ as references, $d_x = 0.05$ as disturbance.

Where, $\Xi_x(s) = \mathcal{L}\{\xi_x(t)\}$, $P_x(s) = \mathcal{L}\{p_x(t)\}$, $D_x(s) = \mathcal{L}\{d_x(t)\}$ denote Laplace transformation. In (16), the absolute value of the coefficient of the CP reference is always greater than the ZMP reference's at $\alpha\beta$. To lead an inverted pendulum to a steady state, the final reference of the CP and the ZMP should be set to the same value. In case of the constant disturbace, the final states of the CP and the ZMP converge to

$$\begin{aligned} &\lim_{s\to 0} s\frac{\Xi_x(s) - \Xi_x^{ref}(s)}{D_x(s)} \\ &= \lim_{s\to 0} s \cdot \frac{\omega(s+g_p)}{(s-\alpha)(s-\beta)} \cdot \frac{1}{s} = \frac{\omega g_p}{\alpha\beta}, \end{aligned} \tag{18}$$

$$\begin{aligned} &\lim_{s\to 0} s\frac{P_x(s) - P_x^{ref}(s)}{D_x(s)} \\ &= \lim_{s\to 0} s \cdot -\frac{(s-\omega)(s+g_p)}{(s-\alpha)(s-\beta)} \cdot \frac{1}{s} = \frac{\omega g_p}{\alpha\beta}. \end{aligned} \tag{19}$$

The same steady errors can be found for the CP and ZMP. The examples for the step responses under constant disturbance are shown in Fig. 4. The CP, the COG, and the ZMP converged to the same position. Although increasing the poles will reduce these steady errors, the peak of the ZMP becomes large according to non-minimum phase property of the inverted pendulum indicated in (16) and (17).

III. Capture Point Error Compensation

A. Capture Point Integration

In order to remove the offset of the state errors, an integration of the Capture Point(CP) is introduced to the controller. The integration of the CP can also be regarded as the component of the state vector. The system in (9) is extended to

$$\frac{\mathrm{d}}{\mathrm{d}t}\begin{bmatrix} \xi_x \\ p_x \\ \int \xi_x dt \end{bmatrix} = \begin{bmatrix} \omega & -\omega & 0 \\ 0 & -g_p & 0 \\ 1 & 0 & 0 \end{bmatrix}\begin{bmatrix} \xi_x \\ p_x \\ \int \xi_x dt \end{bmatrix} + \begin{bmatrix} 0 \\ g_p \\ 0 \end{bmatrix} p_x^d \tag{20}$$

The feedback controller with the CP integration (CPI) is represented as

$$p_x^d = -k_1^{cpi}(\xi_x - \xi_x^{ref}) - k_2^{cpi}(p_x - p_x^{ref}) - k_I^{cpi}\int(\xi_x - \xi_x^{ref})dt \tag{21}$$

Then, the feedback gains can be calculated by the pole assignment.

$$\begin{bmatrix} k_1^{cpi} \\ k_2^{cpi} \\ k_I^{cpi} \end{bmatrix} = \begin{bmatrix} -\frac{\alpha\beta+\beta\gamma+\gamma\alpha-\omega(\alpha+\beta+\gamma-\omega)}{\omega g_p} \\ -\frac{\alpha+\beta+\gamma+g_p-\omega}{g_p} \\ \frac{\alpha\beta\gamma}{\omega g_p} \end{bmatrix} \tag{22}$$

As one of the poles γ is set to 0, the feedback gain in (22) becomes

$$\begin{aligned} k_1^{cpi} &= k_1^{cp} = -\frac{\alpha\beta - \omega(\alpha+\beta-\omega)}{\omega g_p}, \\ k_2^{cpi} &= k_2^{cp} = -\frac{\alpha+\beta+g_p-\omega}{g_p}, \\ k_I^{cpi} &= 0. \end{aligned}$$

We notice these feedback gains are completely the same as the gains resulting from the CP controller in (11). Therefore, the characteristics of this controller can be changed from non-integration to integration of the CP by increasing one of the pole. This implies that it is easy to tune the gains for the CP error compensation by integration.

B. Characteristic of CPI-ZMP controller

Substituting (21) and (22) into the target system in (13), the closed loop transfer function of the CP and the ZMP from the input to the output can be also derived by Laplace transformation, similar to Sec.II-D.

$$\begin{aligned} \Xi_x(s) &= \frac{(\alpha\beta+\beta\gamma+\gamma\alpha-\omega(\alpha+\beta+\gamma-\omega))\,s-\alpha\beta\gamma}{(s-\alpha)(s-\beta)(s-\gamma)} \\ &\quad \times \Xi_x^{ref}(s) \\ &+ \frac{\omega(\alpha+\beta+\gamma-\omega)}{(s-\alpha)(s-\beta)(s-\gamma)}P_x^{ref}(s)) \\ &+ \frac{\omega s(s+g_p)}{(s-\alpha)(s-\beta)(s-\gamma)}D_x(s) \end{aligned} \tag{23}$$

$$P_x(s) = -\left(\frac{s-\omega}{\omega}\right)\Xi_x(s) \tag{24}$$

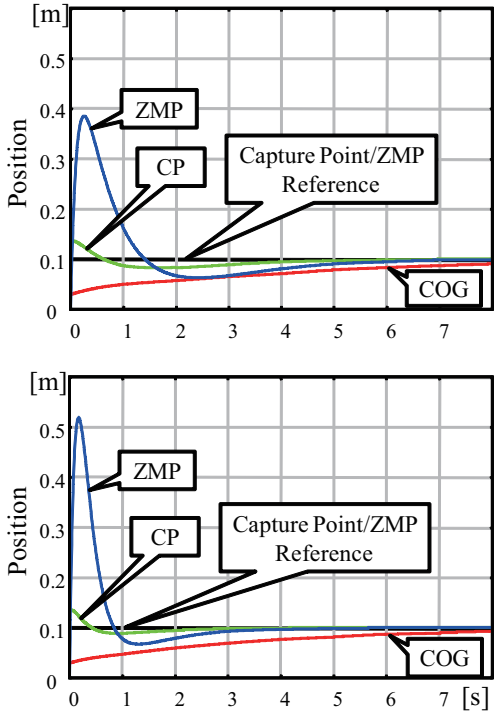

Fig. 5. Step response by CPI controller under presence of disturbance for Pole assignment $\{\alpha, \beta, \gamma\} = (\text{top} : \{-1, -8, -1\}/\text{bottom} : \{-4, -8, -1\})$. The other conditions are same as Fig.4 such as iniaial value.

As the constant disturbance affects the system, the final states of the CP and the ZMP become:

$$\begin{aligned} &\lim_{s\to 0} s\frac{\Xi_x(s) - \Xi_x^{ref}(s)}{D_x(s)} \\ &= \lim_{s\to 0} s \cdot \frac{\omega s(s+g_p)}{(s-\alpha)(s-\beta)(s-\gamma)} \cdot \frac{1}{s} = 0 \end{aligned} \tag{25}$$

$$\begin{aligned} &\lim_{s\to 0} s\frac{P_x(s) - P_x^{ref}(s)}{D_x(s)} \\ &= s \cdot \frac{\omega s(s-\omega)(s+g_p)}{(s-\alpha)(s-\beta)(s-\gamma)} \cdot \frac{1}{s} = 0 \end{aligned} \tag{26}$$

The steady errors of not only the CP but also the ZMP do not remain when the CP integration is applied. The examples of the step responses under constant disturbance are shown in Fig. 5. In contrast to Fig. 4, the CP, the COG and the ZMP converge to the desired reference. While removing the offset, the peak of the ZMP becomes large to compensate the error.

In the actual system, the ZMP should be limited within the support polygon to prevent an unexpected change of the contact on the ground. If the ZMP control output reaches the edge of the support polygon, it is necessary to change the motion to cut this value, eg. by applying landing modification.

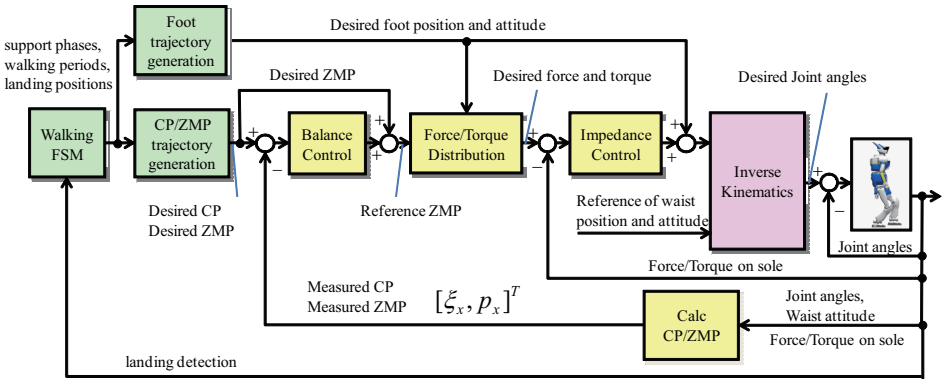

Fig. 6. Walking Control System

IV. Simulation and Experiments

A. Control System

The balance controller is a part of the stabilization functions for a humanoid robot. Our walking control system is shown in Fig.6 [12]. Several feedback loops are implemented in this system. All of feedback loops run at every 1ms. The most inner loop is a position controller at each joint which follows the desired joint angles through the inverse kinematics[13]. This inverse kinematics solves the joint angles from the waist and the feet position and attitude under joint angle and velocity limitations. Then, the impedance controller on each foot brings a reaction force to the desired force at the next inner loop. The desired force is generated through force distribution from the reference ZMP. The reference ZMP is the output of the balance controller added by the desired ZMP as a feedforward term. The desired Capture Point and the desired ZMP are sequentially generated from online biped planner which is composed of the CP-ZMP trajectory generation, the foot trajectory generation and a finite state machine (FSM) of a support phase. The support phase FSM is synchronized with a reaction force which transits from a single support phase to a double support phase. The waist reference is generated through a posture control which tracks the desired waist attitude.

B. Effects of CP integration

To confirm the validity of the proposed controller, the measurement errors of the waist attitude, the COG, the ZMP, and the maximum vertical reaction force with and without the CP integration are compared through experimental walking on flat floor shown in Fig.7 (a)-(d). Each error is evaluated by RMS(root-mean-square) according to walking speed from 0 - 1.57km/h. (a) The waist attitude errors denotes as the roll and the pitch angles around sagittal (x-axis) and lateral (y-axis) direction, respectively. In case of without the CP integration, the pitch angles becomes larger increasing walking speed. In constrast, the waist attitude errors becomes approximately constant with the CP integration. (b) The COG errors are also found the similar responses as the waist attitude errors (a). (c) Although the both sagittal direction of ZMP errors

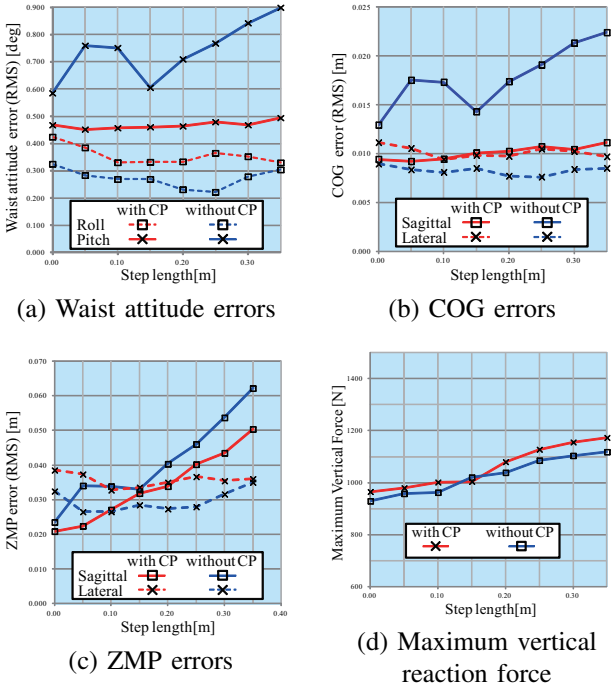

(a) Waist attitude errors (b) COG errors

(c) ZMP errors (d) Maximum vertical reaction force

Fig. 7. Comparion of measurement errors with/without CP integration

with and without the CP integraion becomes larger increasing walking speed, the maximum ZMP error becomes smaller using the CP integration. (d) The maximum vertical reaction force with the CP integration becomes larger a little than without integration.

From (a)-(d), the effects of CP integration can be found for both the ZMP and the COG errors suppression during walkinng, espcesially in sagittal direction in the actual humanoid robot.

C. Walking on Up and Down Slope

To confirm the validity of the proposed controller, in the simulation, we prepare an up and down 10% slope. The snapshots of the walking motion at every 1[s] are shown in Fig.8 The preplanned step length is 0.25[m] and the walking cycle is 0.8[s]. No ground information is given preliminary

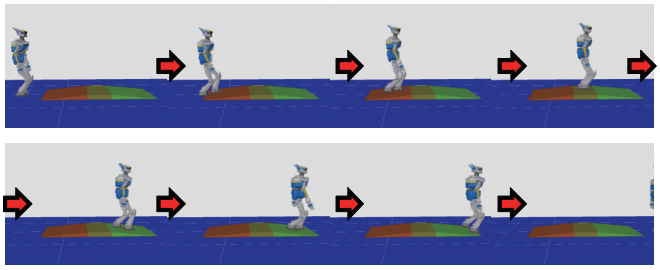

Fig. 8. Walking on 10% slope

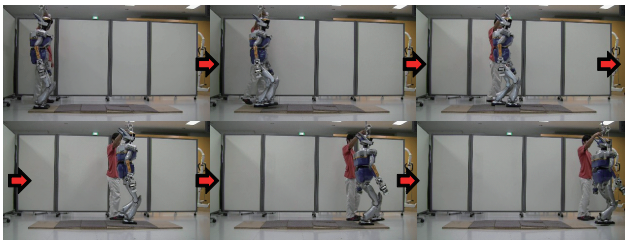

(a) Snap shots

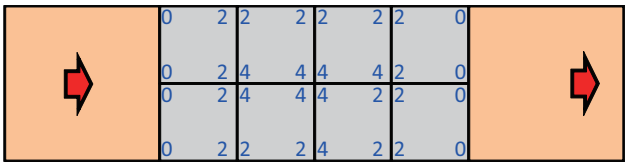

(b) Terrain heights from initial level [cm]

Fig. 9. Experiment of Walking on Uneven Terrain

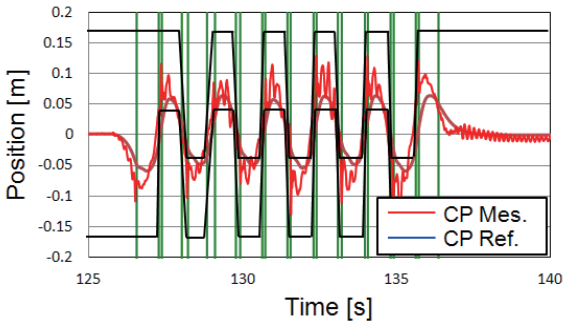

(a) Frontal Plane

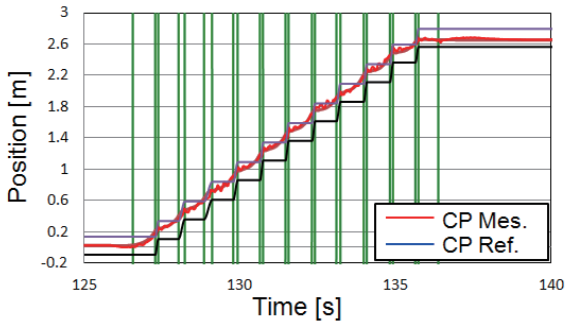

(a) Sagittal Plane

Fig. 10. Desired/Measured Capture Point on Uneven Terrain

for walking. The online COG pattern generator shortens or lengthens a single support period in order to synchronize a sole contact. The humanoid robot can walk on each of the slopes using the proposed controller withoug CP integration with no loss of the transient response as the same as a long term.

D. Experiment

We also performed walking experiments on uneven terrain. The snapshots of the walking experiment at every 2[s] are shown in Fig.9 (a). The terrain heights from the initial level are shown in Fig.9 (b). In this experiment, the preplanned step length is 0.25[m] and the walking cycle is 0.8[s], similar to the simulation. Although the robot didn't keep the center line of the terrain according to an initial orientation or the uncompensated contacts, stable walking could be realized. The desired and measured CP and COG/ZMP are shown in Fig.10 and Fig.11. Although the balance controller does not directly control the COG position, the measure COG position tracked the desired COG position.

The CP error and its integral value are shown in Fig.12. The time response of the CP integration can also be found without divergence. In case of a integral saturation, the wind-up phenomenon will be caused. In this case, the foot modification can avoid this problem.

V. CONCLUSION

In this paper, we improved a balance control base on the Capture Point control (CP). At first a characteristic of the conventional balance controller was shown as the same as the CP controller essentially. Then we analyzed the transfer function of the balance controller. We introduced a new state variable with the CP, its integration and the ZMP in order to trim a long term offset of the CP and the ZMP. The validity of the proposed balance controller was verified through simulation and experiments involving the humanoid robot HRP-2.

According to the support polygon of the feet, a balance controller is subject to restrictions of the upper and lower ZMP value. Biped locomotion has more potential to improve balance capacity by applying foot step modification. That is our future work.

ACKNOWLEDGMENT

Authors would like to thank Nobuyuki Kita, and Shin'ichiro Nakaoka of Humanoid Research Group AIST for their useful advices.

REFERENCES

[1] K. Nishiwaki, and S. Kagami, "High Frequency Walking Pattern Generation based on Preview Control of ZMP," *in Proc. of IEEE Int. Conf. on Robotics and Automation*, pp.2667-2672, 2006.

[2] Y. Choi, D. Kim and B-J.You, "On the Walking Control for Humanoid Robot based on the Kinematic Resolution of CoM Jacobian with Embedded Motion," *in Proc. of IEEE Int. Conf. on Robotics and Automation*, pp.2655-2660, 2006.

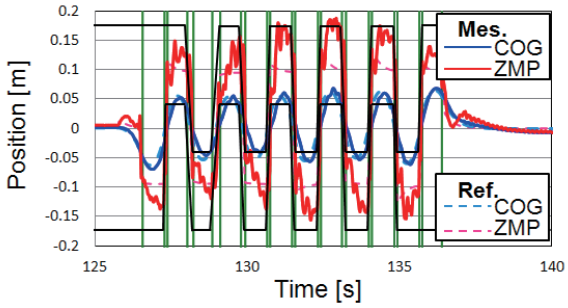

(a) Frontal Plane

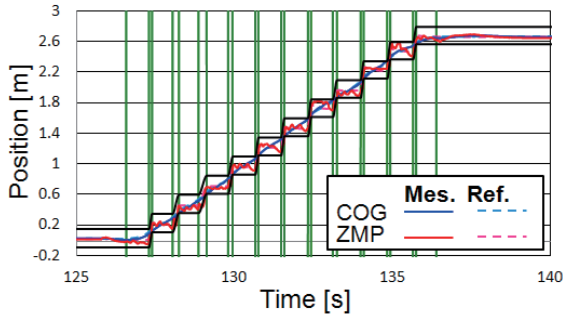

(a) Sagittal Plane

Fig. 11. Desired/Measured COG/ZMP on Uneven Terrain

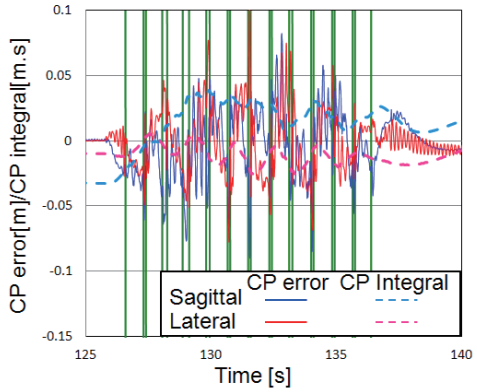

Fig. 12. CP errors and its integral value

[3] P-B. Wieber, "Trajectory free linear model predictive control for stable walking in the presence of strong perturbations," *in Proc. of IEEE-RAS Int. Conf. on Humanoid Robots*, pp.137-142, 2006.

[4] T. Sugihara, "Standing Stabilizability and Stepping Maneuver in Planar Bipedalism based on the Best COM-ZMP Regulator," *in Proc. of IEEE Int. Conf. on Robotics and Automation*, pp.1966-1971, 2009

[5] S. Kajita, M. Morisawa, K. Miura, S. Nakaoka, K. Harada, K. Kaneko, F. Kanehiro, and K. Yokoi, "Biped walking stabilization based on linear inverted pendulum tracking," *in Proc. of IEEE/RSJ Int. Conf. on Intelligent Robots and Systems*, pp.4489-4496, 2010.

[6] K. Miura, M. Morisawa, F. Kanehiro, S. Kajita, K. Kaneko, and K. Yokoi, "Human-like Walking with Toe Supporting for Humanoids," *in Proc. of IEEE/RSJ Int. Conf. on Intelligent Robots and Systems*, pp.4428-4435, 2011.

[7] J. Pratt, J. Carff, S. Drakunov, and A. Goswami, "Capture Point: A Step toward Humanoid Push Recovery," *in Proc. of IEEE-RAS Int. Conf. on Humanoid Robots*, pp.200-207, 2006.

[8] T. Takenaka, T. Matsumoto, T. Yoshiike, T. Hasegawa, S. Shirokura, H. Kaneko and A. Orita, "Real Time Motion Generation and Control for Biped Robot -4th Report: Integrated Balance Control-," *in Proc. of IEEE/RSJ Int. Conf. on Intelligent Robots and Systems*, pp.1601-1608, 2009.

[9] J. Englsberger, C. Ott, M. A. Roa, A. Albu-Schäffer, and G. Hirzinger, "Bipedal walking control based on Capture Point Dynamics," *in Proc. of IEEE/RSJ Int. Conf. on Intelligent Robots and Systems*, pp.4420-4427, 2011.

[10] T. Sugihara, Y. Nakamura, and H. Inoue, "Realtime Humanoid Motion Generation through ZMP Manipulation based on Inverted Pendulum Control," in Proc. of IEEE Int. Conf. on Robotics and Automation, pp.1404-1409, 2002.

[11] K. Kaneko, F. Kanehiro, S. Kajita, H. Hirukawa, T. Kawasaki, M. Hirata, K. Akachi, and T. Isozumi, "The Humanoid Robot HRP2," in Proc. of IEEE Int. Conf. on Robotics and Automation, pp.1083-1090, 2004.

[12] M. Morisawa, F. Kanehiro, K. Kaneko, S. Kajita, K. Yokoi, "Reactive Biped Walking Control for a Collision of a Swinging Foot on Uneven Terrain," *in Proc. of IEEE-RAS Int. Conf. on Humanoids*, pp.768-773, 2011.

[13] F. Kanehiro, W. Suleiman, K. Miura, M. Morisawa, E. Yoshida, "Feasible pattern generation method for humanoid robots," *in Proc. of IEEE-RAS Int. Conf. Humanoid Robots*, pp.542-548, 2009.